Electronic Supporting Information

Polyoxometallates trapped in a zeolitic imidazolate framework leading to high uptake and selectivity of bioactive molecules

Rui Li,[a] Xiaoqian Ren,[a] Jingshu Zhao,[a] Xiao Feng,[a] Xin Jiang,[b] Xinxin Fan,[c] Zhengguo Lin,[a] Xingguo Li,[c] Changwen Hu*[a] and Bo Wang*[a]

[a] *Key Laboratory of Cluster Science, Ministry of Education of China, School of Chemistry, Beijing Institute of Technology, 5 South Zhongguancun Street, Beijing, 100081, P.R. China. E-mail: bowang@bit.edu.cn*

[b] *Spine Surgery, Chinese-Japanese Friendship Hospital, East Yinghua Street, Beijing, 100029, P.R. China.*

[c] *College of Chemistry and Molecular Engineering, Peking University, 5 Yiheyuan Road, Beijing, 100871, P.R. China.*

Table of Contents

S-1. Materials and Instruments.

Materials.

All chemicals were obtained commercially and used without additional purification.

$H_3PW_{12}O_{40}$ *x*H_2O, $H_4SiW_{12}O_{40}$ *x*H_2O, $H_3PMo_{12}O_{40}$ *x*H_2O, ZnO, methyl orange (MO), Rhodamine B (RB), activated carbon, NaCl, KCl, Na_2HPO_4, KH_2PO_4, Ethanol (EtOH) and *N*,*N*-dimethylformamide (DMF) were obtained from Sinopharm Chemical Reagent Co., Ltd, 2-methylimidazole (HMeIM) was purchased from J&K Scientific Company, methylene blue (MB) was used as received from Tianjin JinKe Institute of Fine Chemicals. De-ionized water was used.

Instruments.

Mechanochemical synthetic reactions were carried out in a ball mill (QM-3B, Nanjing University Instrument Factory, China). Adsorption/desorption experiments and MB controlled release were completed in a bath shaker (DSHZ-300A, Taicang Instrument Factory, China). Powder X-ray diffraction (PXRD) patterns of the samples were analyzed with monochromatized Cu-Kα (λ = 1.54178 Å) incident radiation by a Shimadzu XRD-6000 instrument operating at 40 kV voltage and 50 mA current. PXRD patterns were recorded from 5 °to 35 °(2θ) at 298 K. The morphology and size of as-obtained products were investigated using emission scanning electron microscope (SEM, JSM 7500 F) and transmission electron microscope (TEM, JEM-2010). Elemental analyses (C, H, and N) were conducted on Perkin-Elmer 2400 CHN elemental analyzer, Zn, W and Mo were determined by a PLASMA-SPEC (I)

ICP atomic emission spectrometer. The FT-IR spectra were recorded from KBr pellets in the range 400-4000 cm^{-1} on Nicolet 170 SXFT/IR spectrometer. The UV-vis absorption characteristics of the POM anion in the liquid phase were examined on a TU-1901 spectrophotometer in the wavelength range of 200-800 nm. A diffuse reflectance UV-vis spectrum ($BaSO_4$ pellets) was obtained from the solid state with a Varian Cary 500 UV-vis-NIR spectrometer. N_2 isotherm was measured using a Builder SSA-4200 automatic volumetric gas adsorption analyzer.

S-2. Synthetic methods.

Mechanochemical synthetic reactions were carried out in a ball mill using a 50 mL stainless steel grinding jar and 5 steel balls with 10 mm diameter. Zinc oxide (5 mmol) and HMeIM (10 mmol) with $H_3PW_{12}O_{40}$ xH_2O, $H_4SiW_{12}O_{40}$ xH_2O, or $H_3PMo_{12}O_{40}$ xH_2O (0.2-1.6 mmol) were added into the jar, along with 1 mL ethanol, then the mixture was ground for 30 min at 40 Hz. The solids were collected and washed with large amounts of ethanol and de-ionized water, stirred and ultra-sonicated until there is no POM anions were present in the solution as evidence by UV-vis spectroscopy. The solids were dried at 60 ℃ overnight and powders were obtained.

S-3. Experimental and simulated PXRD patterns.

The PXRD patterns of materials before and after each washing-soaking cycles were compared with that of the original ZIF-8, the good agreement of the peaks throughout the diagrams demonstrates that the BITs are chemically stable.

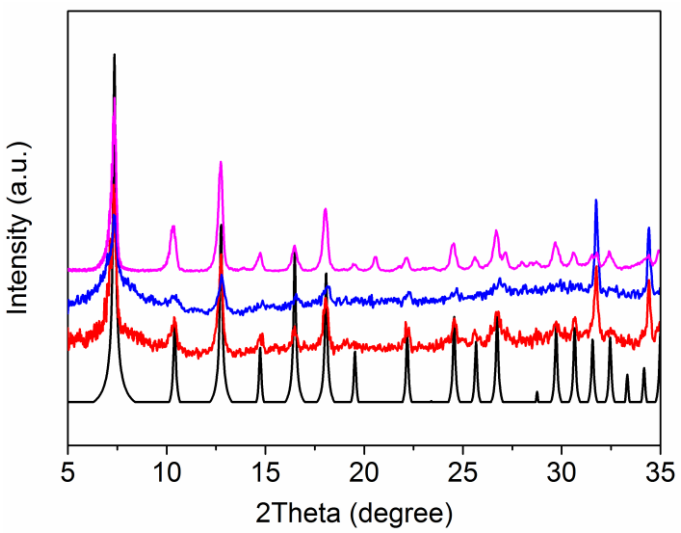

Figure S1. PXRD patterns of simulated ZIF-8 (black), as-synthesized BIT-1 (red), as-synthesized BIT-2 (blue) and as-synthesized BIT-3 (pink).

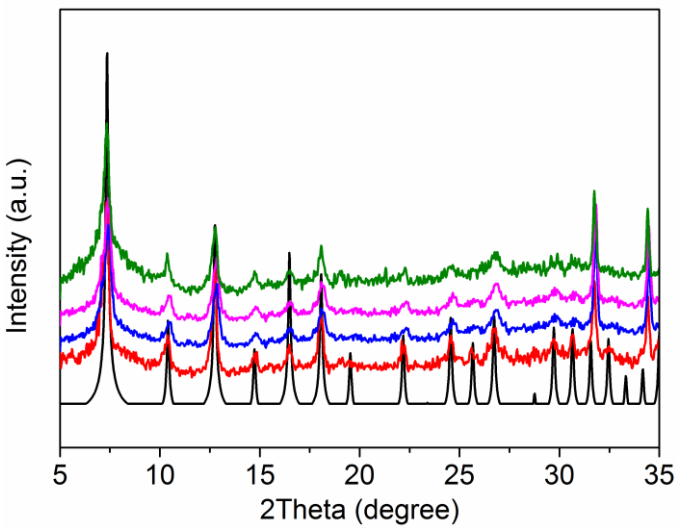

Figure S2. PXRD patterns of simulated ZIF-8 (black), as-synthesized BIT-1 (red), BIT-1 soaked in H_2O (blue), EtOH (pink), DMF (green) for 7 days.

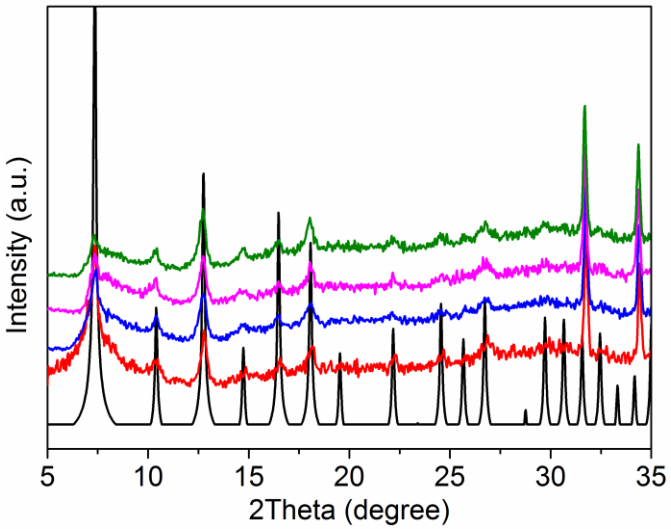

Figure S3. PXRD patterns of simulated ZIF-8 (black), as-synthesized BIT-2 (red), BIT-2 soaked in H_2O (blue), EtOH (pink) and DMF (green) for 7 days.

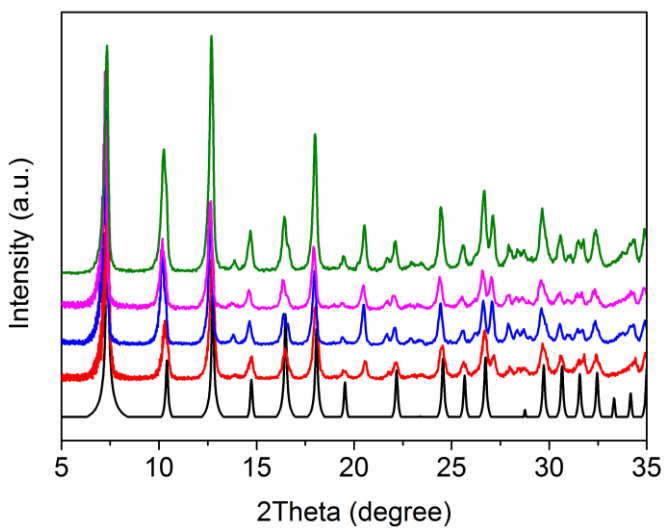

Figure S4. PXRD patterns of simulated ZIF-8 (black), as-synthesized BIT-3 (red) and BIT-3 soaked in H_2O (blue), EtOH (pink) and DMF (green) for 7 days.

S-4. Leaching test, and UV-vis and FT-IR spectroscopy of samples.

Samples (10 mg) were immersed in 5 mL H_2O, EtOH and DMF, respectively. After 7 days, solutions were measured by liquid-phase UV-vis. Solids were collected and dried, then measured by diffuse reflectance UV-vis and FT-IR.

The diffuse reflectance UV-vis spectra indicated that the three samples and the

solids after leaching test displayed absorption peaks in 370 nm and 260-270 nm, corresponding to absorption peak ZIF-8 and POMs, respectively, which suggests the presence of POMs inside ZIFs. Meanwhile, the liquid-phase UV-vis spectroscopy of the solution after 7 days soaking confirmed that there were no POM anions leaching out from the BITs.

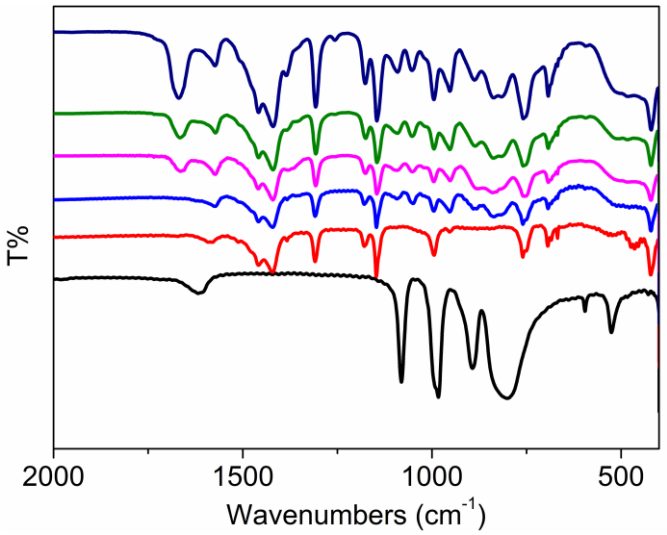

Figure S5. FT-IR spectra of $H_3PW_{12}O_{40}$, ZIF-8 and BIT-1. Black, $H_3PW_{12}O_{40}$; Red, ZIF-8; Blue, BIT-1 as-synthesized; Pink, Green and Purple are BIT-1 soaked in H_2O, EtOH and DMF for 7 days, respectively. FT-IR (KBr, cm^{-1}) for $H_3PW_{12}O_{40}\subset$ZIF-8 (BIT-1): 1667, 1458, 1422, 1308, 1146, 1051, 995, 952, 886, 836, 759, 693.

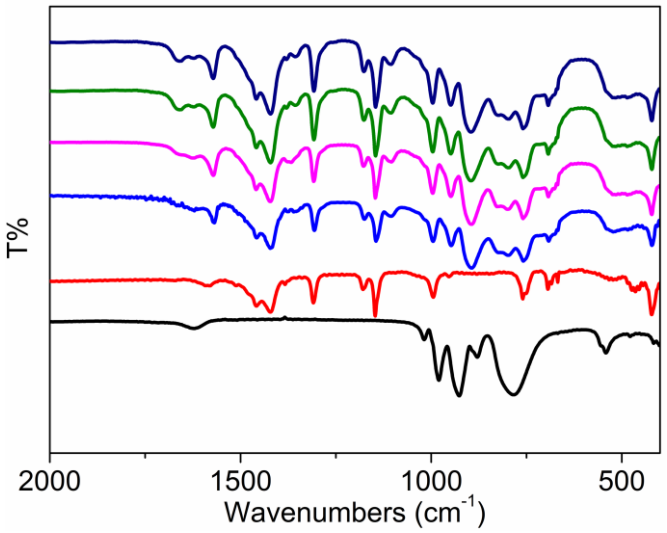

Figure S6. FT-IR spectra of $H_4SiW_{12}O_{40}$, ZIF-8 and BIT-2. Black, $H_4SiW_{12}O_{40}$; Red, ZIF-8; Blue, BIT-2 as-synthesized; Pink, Green and Purple are BIT-2 soaked in H_2O, EtOH and DMF for 7 days, respectively. FT-IR (KBr, cm^{-1}) for $H_3SiW_{12}O_{40}\subset$ZIF-8 (BIT-2): 1569, 1458, 1423, 1307, 1146, 1105, 995, 948, 894, 798, 759, 692.

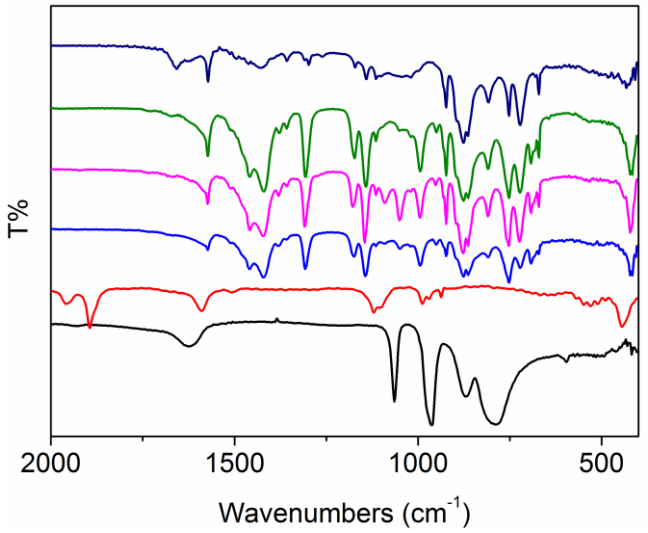

Figure S7. FT-IR spectra of $H_3PMo_{12}O_{40}$, ZIF-8 and BIT-3. Black, $H_3PMo_{12}O_{40}$; Red, ZIF-8; Blue, BIT-3 as-synthesised; Pink, Green and Purple are BIT-3 soaked in H_2O, EtOH and DMF for 7 days, respectively. FT-IR (KBr, cm^{-1}) for $H_3PMo_{12}O_{40}\subset$ZIF-8 (BIT-3): 1573, 1458, 1421, 1307, 1143, 1049, 994, 924, 876, 809, 752, 692.

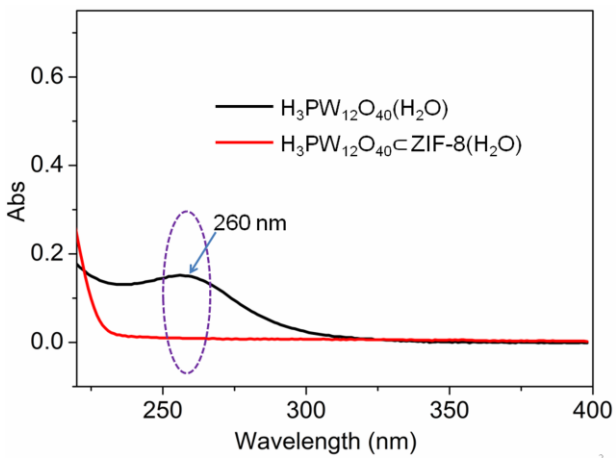

Figure S8. Liquid-phase UV-vis spectra from leaching test of BIT-1 in H_2O.

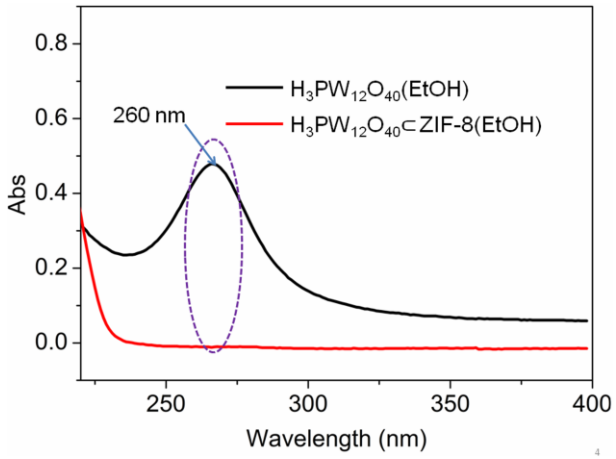

Figure S9. Liquid-phase UV-vis spectra from leaching test of BIT-1 in EtOH.

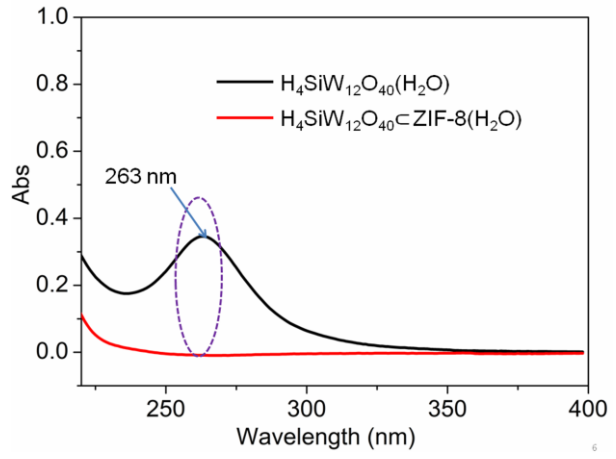

Figure S10. Liquid-phase UV-vis spectra from leaching test of BIT-2 in H_2O.

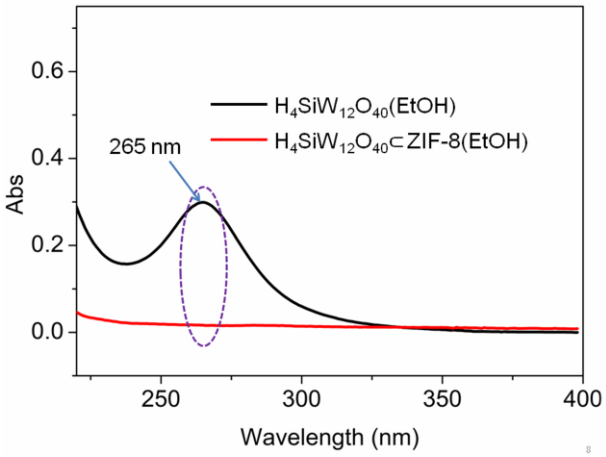

Figure S11. Liquid-phase UV-vis spectra from leaching test of BIT-2 in EtOH.

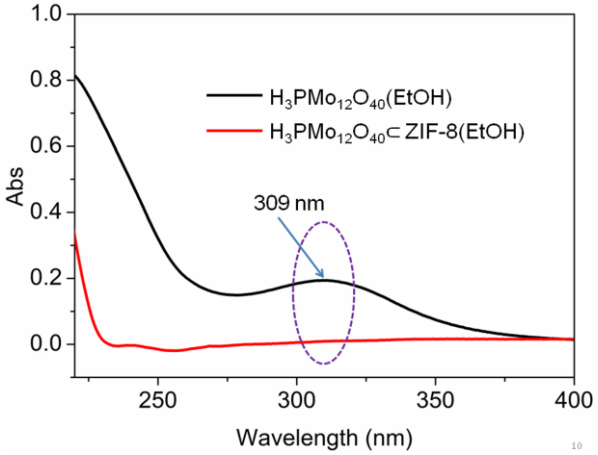

Figure S12. Liquid-phase UV-vis spectra from leaching test of BIT-3 in EtOH.

S-5. Elemental analyses.

Elemental Anal. Calcd (Found%) for $[Zn(C_4H_5N_2)_2]_8(H_3PW_{12}O_{40})$: Zn, 11.11 (11.11); W, 47.13 (46.79); C, 16.41 (13.06); H,1.43 (1.82); N, 9.57 (7.65).

Elemental Anal. Calcd (Found%) for $[Zn(C_4H_5N_2)_2]_9(H_4SiW_{12}O_{40})$: Zn, 11.93 (12.14); W, 44.97 (43.89); C, 17.61 (15.37); H,1.47 (1.58); N, 10.28 (8.12).

Elemental Anal. Calcd (Found%) for $[Zn(C_4H_5N_2)_2]_8(H_3PMo_{12}O_{40})$: Zn, 14.34 (13.34); Mo, 31.76 (30.50); C, 21.19 (17.67); H,1.85 (1.47); N, 12.36 (8.96).

Table S1. The results of different POM loadings by controlling the amount of POM.

entry	starting materials ratio $n(H_3PW_{12}O_{40})/n(Zn)$	experimental results $n(W)/n(Zn)$	products	yield (Zn) (%)
1	1: 24	12: 59	$[Zn(MeIM)_2]_{59}(H_3PW_{12}O_{40})$	58.0
2	1:12	12:16	$[Zn(MeIM)_2]_{16}(H_3PW_{12}O_{40})$	55.8
3	1:6	12:8	$[Zn(MeIM)_2]_8(H_3PW_{12}O_{40})$	27.1
4	1:3	12:8	$[Zn(MeIM)_2]_8(H_3PW_{12}O_{40})$	27.1

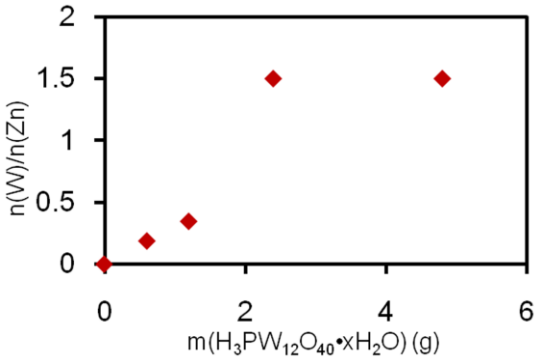

Figure S13. n(W)/n(Zn) with the increase of the amount of POM.

S-6.Gas adsorption analyses.

These four BIT-3 samples are all porous with an apparent BET surface area of 1360, 1290, 1040 and 940 $m^2\ g^{-1}$ were obtained with different POM loadings by using the data points on the adsorption branch of the N_2 isotherm in the range P/P_0 = 0.05-0.25.

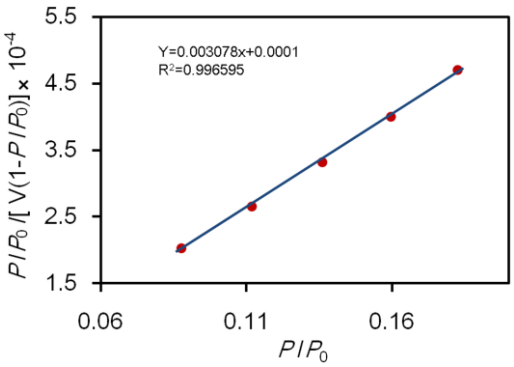

Figure S14. Langmuir equation fitting curve for ZIF-8 N_2 isotherm (adsorption branch data points, P/P_0 = 0.05–0.25). Surface area 1460 m^2 g^{-1}, linearity 0.9966.

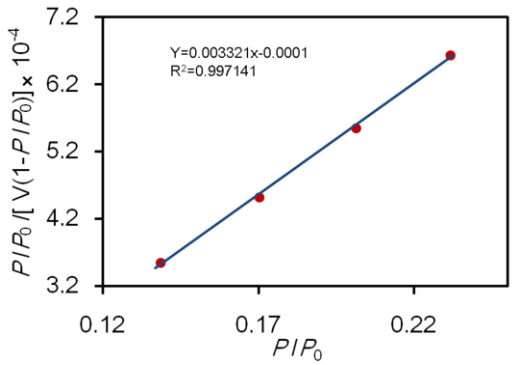

Figure S15. Langmuir equation fitting curve for $[Zn(C_4H_5N_2)_2]_{380}(H_3PMo_{12}O_{40})$ N_2 isotherm (adsorption branch data points, P/P_0 = 0.05–0.25). Surface area 1360 m^2 g^{-1}, linearity 0.9971.

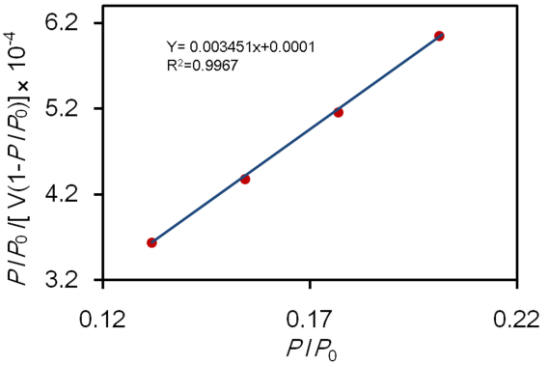

Figure S16. Langmuir equation fitting curve for $[Zn(C_4H_5N_2)_2]_{102}(H_3PMo_{12}O_{40})$ N_2 isotherm (adsorption branch data points, P/P_0 = 0.05–0.25). Surface area 1290 m^2 g^{-1}, linearity 0.9967.

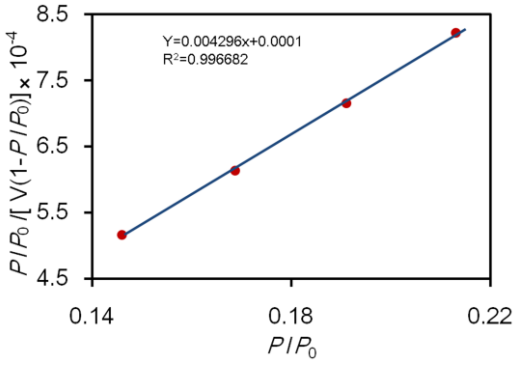

Figure S17. Langmuir equation fitting curve for $[Zn(C_4H_5N_2)_2]_{86}(H_3PMo_{12}O_{40})$ N_2 isotherm (adsorption branch data points, P/P_0 = 0.05–0.25). Surface area 1040 m^2 g^{-1}, linearity 0.9967.

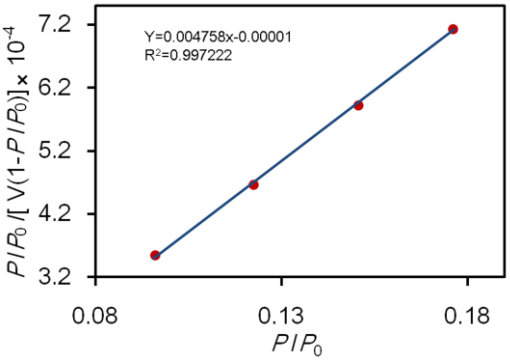

Figure S18. Langmuir equation fitting curve for $[Zn(C_4H_5N_2)_2]_{54}(H_3PMo_{12}O_{40})$ N_2 isotherm (adsorption branch data points, P/P_0 = 0.05–0.25). Surface area 940 m^2 g^{-1}, linearity 0.9972.

According to elemental analysis data, the molecular formula of BIT-3 with different POM loadings are $[Zn(C_4H_5N_2)_2]_{380}(H_3PMo_{12}O_{40})$, $[Zn(C_4H_5N_2)_2]_{102}(H_3PMo_{12}O_{40})$, $[Zn(C_4H_5N_2)_2]_{86}(H_3PMo_{12}O_{40})$, and $[Zn(C_4H_5N_2)_2]_{54}(H_3PMo_{12}O_{40})$. One SOD cage of ZIF-8 consists of 6 zinc atoms. Thus for each molecular formula of four BIT-3 samples, there are 63 (380/6), 17 (102/6), 14 (86/6) and 9 (54/6) SOD cages, respectively. Each POM cage occupied one out of every 63, 17, 14 and 9 SOD cages in the pristine ZIF-8, leaving 62, 16, 13

and 8 cages accessible for gas molecules. We could assume the volume factors are 0.9841 (62/63), 0.9411 (16/17), 0.9286 (13/14) and 0.8889 (8/9). Accordingly the mass factors (the mass contribution of POMs) are 0.9513, 0.9252, 0.7793 and 0.7402. Then the multiplication of mass factor and volume factor should be 0.9362, 0.8708, 0.7236 and 0.6580. When the BET surface area of the pristine ZIF-8, 1460 m^2 g^{-1}, times 0.9362, 0.8708, 0.7236, and 0.6580, respectively, we then get 1365 m^2 g^{-1}, 1270 m^2 g^{-1}, 1055 m^2 g^{-1}, 960 m^2 g^{-1} as the theoretical BET surface areas. They are very close to the experimental BET surface areas, 1360, 1290, 1040, and 940 m^2 g^{-1}, respectively. However, when we simply assumed the POMs only contributed to the total mass of each sample without occupying any cages, the surface area calculations turned to be 1388, 1350, 1137 and 1080 m^2 g^{-1}, which were far off the experimental data.

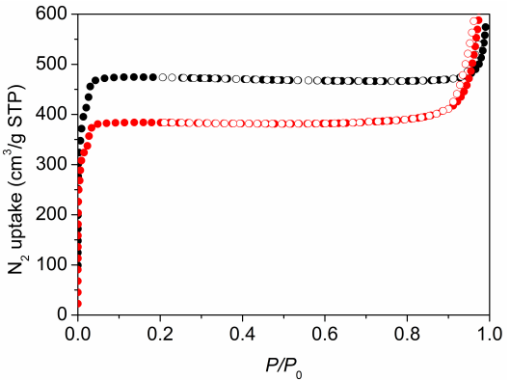

Figure S19. Gas adsorption/desorption isotherms of $H_3PW_{12}O_{40}$⊂ZIF-8 (BIT-1) for N_2 (77 K). Black, red, for ZIF-8 and $[Zn(C_4H_5N_2)_2]_{95}(H_3PW_{12}O_{40})$, respectively. The filled circles represent adsorption branches and open circles represent desorption ones.

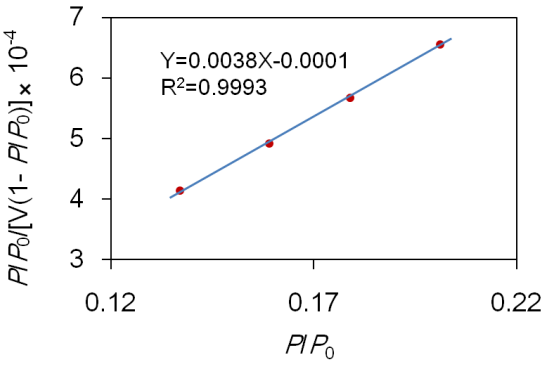

Figure S20. Langmuir equation fitting curve for $[Zn(C_4H_5N_2)_2]_{95}(H_3PW_{12}O_{40})$ N_2 isotherm (adsorption branch data points, P/P_0 = 0.05–0.25). Surface area 1190 m^2 g^{-1}, linearity 0.9993.

S-7. TEM and SEM images.

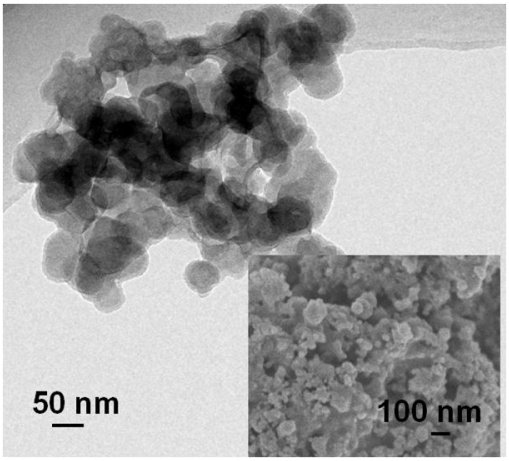

Figure S21. TEM and SEM images of BIT-1.

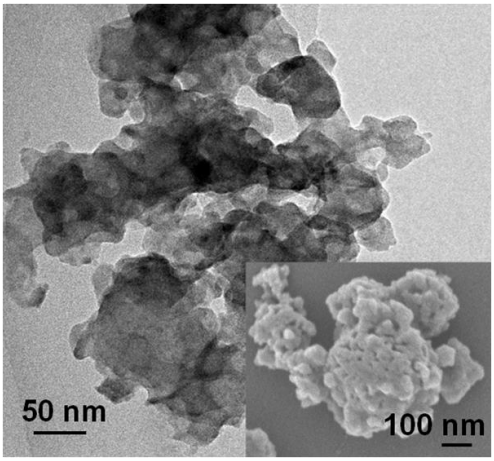

Figure S22. TEM and SEM images of BIT-2.

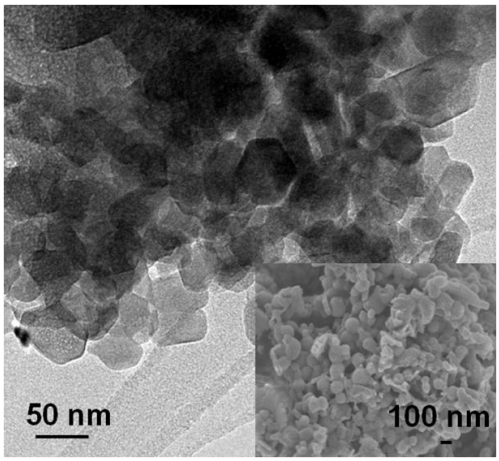

Figure S23. TEM and SEM images of BIT-3.

S-8. Adsorption experiments.

The calibration plots of dyes.

An aqueous stock solution of MB, MO or RB was prepared by dissolving MB in deionized water, respectively. Aqueous solutions with different concentration of MB, MO or RB (2–20 mg L^{-1}) were prepared by successive dilution of the solution with water. The calibration plots were generated by using several dye solutions with different concentrations.

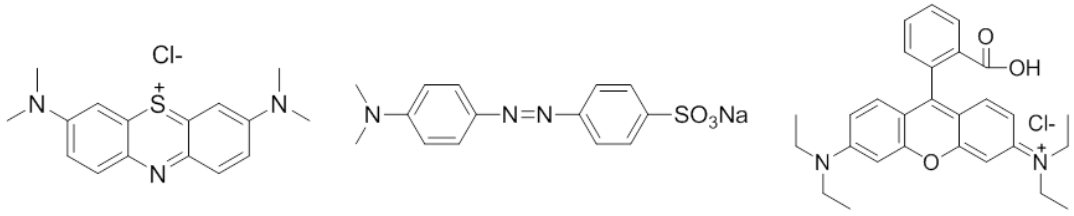

methylene blue methyl orange Rhodamine B

Figure S24. The structures of dye molecules methylene blue (MB), methyl orange (MO) and Rhodamine B (RB).

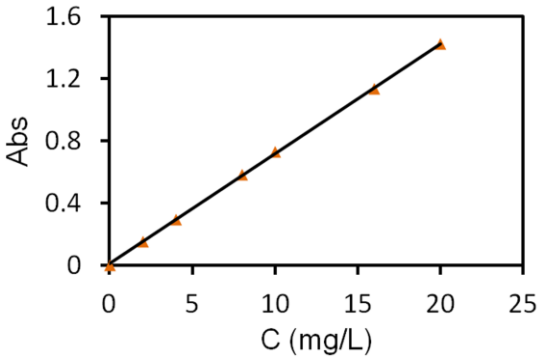

Figure S25. The calibration plots of MO (H_2O).

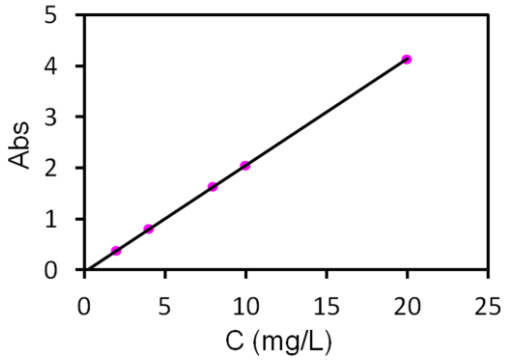

Figure S26. The calibration plots of RB (H_2O).

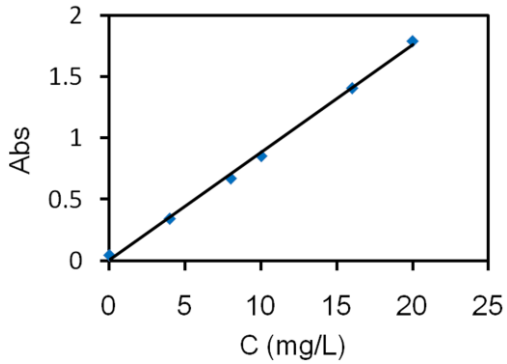

Figure S27. The calibration plots of MB (H_2O).

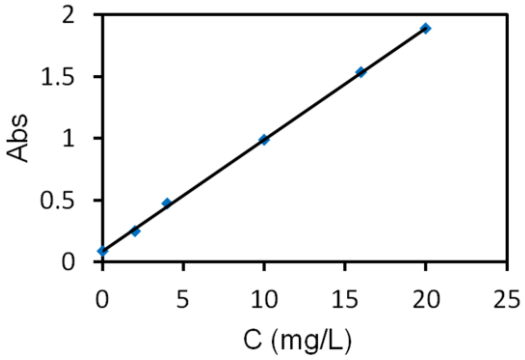

Figure S28. The calibration plots of MB (SBF, pH 7.4).

Dye Adsorption equilibrium experiments.

Adsorption equilibrium experiments were carried out by adding BIT-1 (20 mg) in 100 mL of MB aqueous solution with varied concentration (40-200 mg L^{-1}) at room temperature and shaken at 180 rpm. After 2 h the suspension was centrifugated and the final concentration of MB in solution was measured by UV-vis spectrometer at λ_{max} of 664 nm for MB. The specific adsorbed amount of MB was calculated according to the equation:

$Q_e = V(C_0 - C_e)/m$

where C_0 and C_e are the initial and equilibrium liquid-phase concentrations of MB (mg L^{-1}), m is the amount of adsorbent (g), and V is the volume of the solution (L).

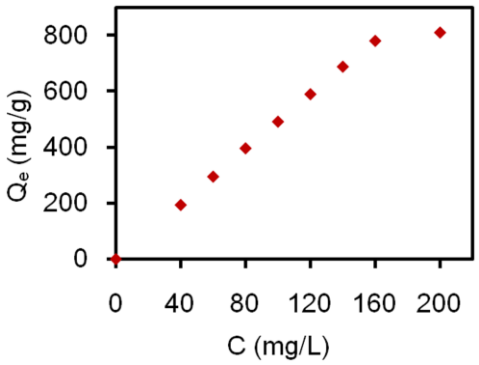

Figure S29. Adsorption isotherm of MB onto $H_3PW_{12}O_{40}$⊂ZIF-8 at 298 K.

Dye adsorption kinetic experiments.

The procedures of kinetic experiments were basically identical to those of equilibrium tests. Kinetic analysis of MB adsorption was performed by adding 10 mg samples include BIT-1, ZIF-8 or activated carbon respectively into 50 mL of MB aqueous solution with concentration 60 mg L^{-1} at room temperature and shaken at 180 rpm. The aqueous samples were taken at preset time intervals, and the concentrations of dyes were similarly measured.

Dye adsorption selective kinetic experiments.

The procedures of selective kinetic experiments were basically identical to those of kinetic experiments. BIT-1 (5 mg) was added into 50 mL of MB, MO or RB aqueous solution with concentration 20 mg L^{-1} respectively at room temperature and shaken at 180 rpm. The aqueous samples were taken at preset time intervals, and the concentrations of dyes were similarly measured. UV-vis adsorption spectra were recorded at different intervals to monitor the adsorption process. The concentrations of dyes were determined through a UV-vis spectrometer at the maximum adsorbance of each dye (664 nm, 464 nm and 554 nm for MB, MO and RB, respectively).

BIT-1 (5 mg) was also added into 50 mL mixed aqueous solution of MB and MO, or MB and RB with concentration 20 mg L^{-1} respectively at room temperature and shaken at 180 rpm. The aqueous samples were taken at preset time intervals, and the concentrations of dyes were similarly measured.

Dye desorption experiments.

BIT-1 (100 mg) was added into 50 mL of MB aqueous solution with concentration 10 mg L^{-1} at room temperature and shaken at 180 rpm. The solids were collected and dried, followed by stirring and washing with 100 mL NaCl (1 g L^{-1}) solution in ethanol/water mixture (volume ratio of 1:1) for 3 times. Recovered white solid (20 mg) was carried out adsorption test in 50 mL MB aqueous solution with concentration 10 mg L^{-1} again.

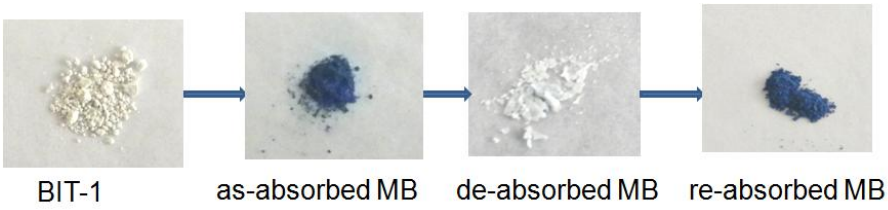

Figure S30. Photos of BIT-1 adsorption and recycled.

S-9. MB Controlled Release.

Solids (100 mg) which adsorbed MB was soaked in a simulated body fluid (SBF, pH 7.4) at 37 ℃ and shaken at 80 rpm. The simulated body fluid includes NaCl, KCl, Na_2HPO_4 and KH_2PO_4. At different times, 3 mL of the solution from the vial was removed and 3 mL of fresh SBF buffer was added to the vial. The releasing process was monitored and calculated by liquid-phase UV-vis spectroscopy.

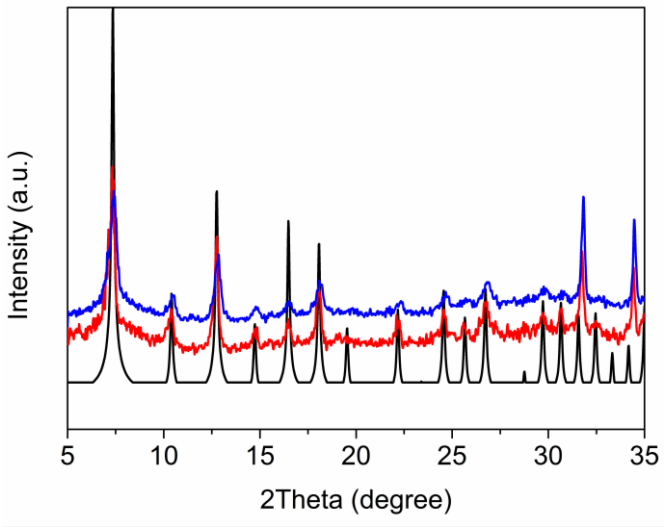

Figure S31. PXRD patterns of simulated ZIF-8 (black), as-synthesized BIT-1 (red) and after MB Controlled Release (blue).

S-10. 5-FU controlled release.

BIT-1 was mechanochemically synthesized using ZnO (5 mmol, 0.407 g), HMeIM (10 mmol, 0.821 g) and $H_3PW_{12}O_{40}$ $x$$H_2O$ (0.2 mmol, 0.600 g). ZIF-8 was mechanochemically synthesized using ZnO (5 mmol, 0.407 g) and HMeIM (10 mmol,

0.821 g). ZIF-8 was solvothermally synthesized using $Zn(NO_3)_2 \cdot 6H_2O$ (1.2 mmol, 0.350 g) and HMeIM (2.4 mmol, 0.200 g) dissolved in 15 mL DMF and three drops HNO_3, then heated at 120 ℃ for 24 hours. BIT-1 (1.3 g) and 5-FU (0.1 g) were ground in a ball mill and the solids were then collected and washed with EtOH to get rid of the excessive 5-FU. Then the solids were dried at 60 ℃. ZIF-8 carried 5-FU used the same way.15 mg of thus obtained BIT-1 powders loaded with 1.375 mg of 5-FU (9.2% as evidenced by elemental analyses) was soaked in a simulated body fluid (SBF, pH 7.4) at 37 ℃ and shaken at 80 rpm. At certain time intervals, 3 mL of the solution from the vial was removed and 3 mL of fresh SBF buffer was added to the vial. The releasing process was monitored and calculated by liquid phase UV-vis spectroscopy at λ_{max} of 266 nm for 5-FU. In comparison, ZIF-8 samples that were synthesized mechanically and solvothermally, were also tested in the controlled release experiments under the same conditions.

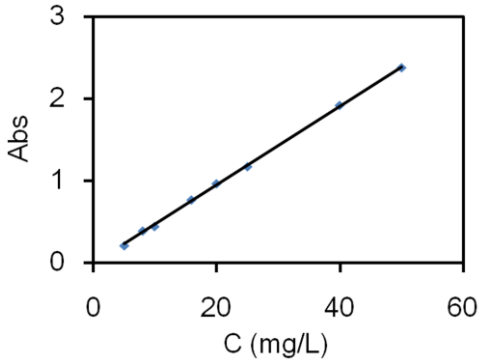

Figure S32. The calibration plots of 5-FU (SBF, pH 7.4).

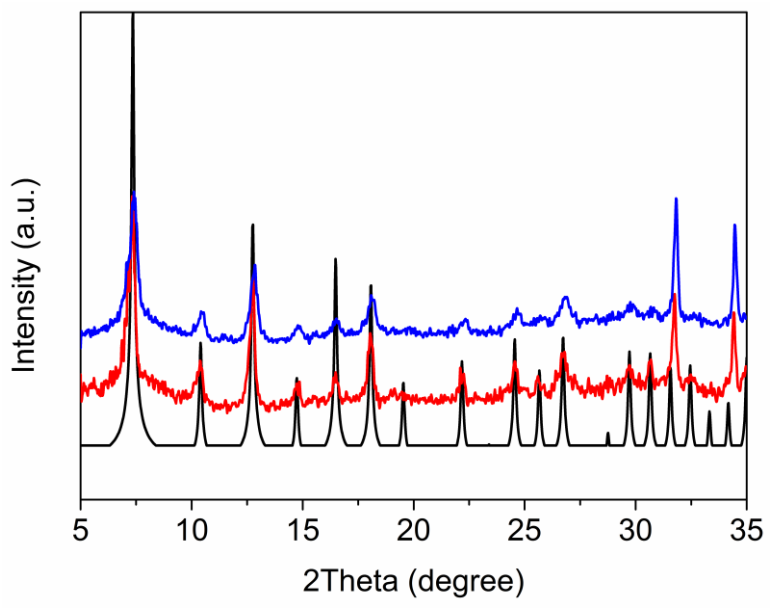

Figure S33. PXRD patterns of simulated ZIF-8 (black), as-synthesized BIT-1 (red) and after 5-FU Controlled Release (blue).

References

[s1] Zou, C.; Zhang, Z. J.; Xu, X.; Gong, Q. I.; Li, J.; Wu, C. D. *J. Am. Chem. Soc.* **2012**, *134*, 87.

[s2] Liu, F.; Chung, S.; Oh, G.; Seo, T. S. *ACS Appl. Mater. Inter.* **2012**, *4*, 922.

[s3] The national standard of the People's Republic of China: Wooden granular activated carbon for water purification. GB/T13803.2-1999.